Applied Biochemistry and Biotechnology (2019) 189:1141–1155
https://doi.org/10.1007/s12010-019-03053-7

Engineering D-Lactate Dehydrogenase from *Pediococcus acidilactici* for Improved Activity on 2-Hydroxy Acids with Bulky C_3 Functional Group

Hoe-Suk Lee[1] · Jisu Park[2] · Young Je Yoo[1,3] · Young Joo Yeon[2]

Received: 28 January 2019 / Accepted: 22 May 2019 /
Published online: 13 June 2019

Abstract

Engineering D-lactic acid dehydrogenases for higher activity on various 2-oxo acids is important for the synthesis of 2-hydroxy acids that can be utilized in a wide range of industrial fields including the production of biopolymers, pharmaceuticals, and cosmetic compounds. Although there are many D-lactate dehydrogenases (D-LDH) available from a diverse range of sources, there is a lack of biocatalysts with high activities for 2-oxo acids with large functional group at C_3. In this study, the D-LDH from *Pediococcus acidilactici* was rationally designed and further engineered by controlling the intermolecular interactions between substrates and the surrounding residues via analysis of the active site structure of D-LDH. As a result, Y51L mutant with the catalytic efficiency on phenylpyruvate of 2200 s^{-1} mM^{-1} and Y51F mutant on 2-oxobutryate and 3-methyl-2-oxobutyrate of 37.2 and 23.2 s^{-1} mM^{-1} were found, which were 138-, 8.5-, and 26-fold increases than the wild type on the substrates, respectively. Structural analysis revealed that the distance and the nature of the interactions between the side chain of residue 51 and the substrate C_3 substituent group significantly affected the kinetic parameters. Bioconversion of phenyllactate as a practical example of production of the 2-hydroxy acids was investigated, and the Y51F mutant presented the highest productivity in in vitro conversion of D-PLA.

Electronic supplementary material The online version of this article (https://doi.org/10.1007/s12010-019-03053-7) contains supplementary material, which is available to authorized users.

✉ Young Je Yoo
yjyoo@snu.ac.kr

✉ Young Joo Yeon
yjyeon@gwnu.ac.kr

Extended author information available on the last page of the article

Keywords D-Lactate dehydrogenase · 2-Hydroxy acids · Substrate specificity · Rational design · Computational docking

Introduction

D-Lactate dehydrogenase (D-LDH, EC number 1.1.1.28), a member of D-isomer-specific 2-hydroxy acid dehydrogenase family with a common Rossmann fold, has been implicated in the reduction of 2-oxo acids to their corresponding stereospecific D-2-hydroxy acids, which include industrially important compounds such as D-lactate, D-phenyllactate (PLA), D-2-hydroxybutyrate, and D-3-methyl-2-hydroxybutyrate, for uses as precursors to biopolymers, pharmaceuticals, and cosmetic compounds (Supplementary Fig. 1a) [1–6]. Recent focus was on PLA with antimicrobial activity against deteriorating fungi and bacteria, such as *Aspergillus ochraceus*, *Staphylococcus aureus*, and certain strains of *E. coli* [7]. Since it is found naturally in honey and fermented food, and can be synthesized in Generally Recognized As Safe (GRAS) microorganism such as *Lactobacillus* and *Pediococcus* species, it is regarded to be a potent biopreservative in foods [8]. D-LDHs cloned from various species were subjected to kinetic and/or bioconversion studies for the synthesis of PLA from phenylpyruvate (PPA), including *L. pentosus*, *L. bulgaricus*, *P. pentosaceus*, and *P. acidilactici* [9–14].

Since D-LDHs have preference for pyruvate over other 2-oxo acids, the substrate specificity of the enzyme can be changed to expand its applicability on PPA and other 2-oxo acids via protein engineering [13, 14]. Rational design approaches via structural comparisons between different enzymes or molecular docking are often used to change the active site befitting the target substrates with varying sizes of substituent groups [15–17]. The structure-function relationship–based method can be used in the prediction and analysis of the substrate binding affinity and orientation. Structural studies on D-LDHs based on the X-ray crystal structures of *L. bulgaricus* (PDB, 1j49), *L. helveticus* (PDB, 2DLD), and *Aquifex aeolicus* (PDB, 3KB6) revealed they are homodimers where each subunit consists of a catalytic domain and a cofactor binding domain, and the active site located in the inter-domain cleft [18, 19]. The cofactor binding domain contains a bound cofactor NADH and H295 for donating a hydride to the C_2 and 2-oxo functional group of the substrate in reductive reaction (Supplementary Fig. 1b, the residue numbering follows those of *P. acidilactici* D-LDH). The catalytic domain side of the active site comprises of a carboxylic acid–stabilizing loop (N76-G78) and Y100. The hydride transfer distances d_1 (between the cofactor NADH and C_2 of the substrate) and d_2 (between H295 Nε and 2-oxo group) are known to affect the activation energy and therefore k_{cat} of the reaction [20]. R234 in the same domain stabilizes the 2-oxo and one of the carboxylic oxygen of the substrate.

Rational designs of D-LDHs to change its substrate specificity in favor of PPA have been made in *L. pentosus*, *L. bulgaricus*, and *Sporolactobacillus inulinus* [9–12, 21]. Comparison of the structures of *L. bulgaricus* D-LDH and *L. casei* D-2-hydroxyisocaproate dehydrogenase revealed Y53 (corresponding to Y51 in paLDH) can be a key substrate discriminating factor in the D-LDHs from *L. bulgaricus* and *L. pentosus* [11, 12, 22]. In another study, docking of PPA in the active site of *S. inulinus* D-LDH was employed to select mutation candidates nearby [21].

In this study, *P. acidilactici* D-LDH (paLDH) has been subjected to the rational design and docking analysis for PPA and other 2-oxo acids with C_3 functional groups bulkier than pyruvate. The paLDH is one of the wild type D-LDHs from lactic acid bacteria that has the highest activity on PPA, yet there has been no docking study or engineering attempt so far [13, 23]. The enzyme also has high sequence identities as other D-LDHs, allowing homology modeling and rational design.

Material and Methods

Material

The paLDH sequence (NCBI accession: WP_002831533) was commercially synthesized with C-terminal His_6 tag and codon optimization for expression in *Escherichia coli* from GenScript (NJ, USA). Restriction enzymes were purchased from Enzynomics (Daejeon, Korea). Mutation primer synthesis and sequencing of the resulting paLDH mutants were performed by Cosmogenetech (Seoul, Korea). Competent *E. coli* DH5α and BL21(DE3) were purchased from Invitrogen (Carlsbad, CA). PPA was purchased from Tokyo Chemical Industry (Tokyo, Japan). Pyruvate, 2-oxobutyrate (OB), 3-methyl-2-oxobutyrate (MOB), and all other chemicals were purchased from Sigma-Aldrich (St. Louis, USA).

Rational Design of paLDH and Substrate Docking

The structure of paLDH was homology modeled based on the D-LDH from *L. bulgaricus* (PDB, 1j49) with the highest sequence identity, found by the position-specific iterated-BLAST [18, 24]. The homology modeling follows the protocol of the Prime software from Schrödinger, where the secondary structures are predicted and aligned with the template before energy-based structure minimization [25]. The bound NAD was changed to NADH to mimic the substrate binding state and energy minimization. Mutant structures were created from the homology model by mutate residue function in 3D builder followed by prime minimization. The quality of the model was validated by Saves server v5.0 (University of California Los Angeles, LA, USA) [26, 27]. The substrates were prepared as ligands for docking via LigPrep, all possible ionization states [28]. Glide software was then used for the docking of the substrate in the homology model [29–31]. A grid was generated to encompass the active site of paLDH including the nicotinamide moiety of the cofactor and catalytic H295, and the Standard Precision mode of Glide was used to produce docking poses of the substrates.

Site-Directed Mutagenesis, Protein Expression, and Purification

The synthetic paLDH gene was cloned into pET22b(+) vector between NdeI and XhoI restriction sites, in order to transform into *E. coli* DH5α for cloning and mutation, and *E. coli* BL21 (DE3) for protein expression. The gene was mutated with the primers described in the Supplementary Table S1 following the QuikChange II Site-Directed Mutagenesis protocol (Agilent, Santa Clara, USA) [32]. The *E. coli* cells transformed with wild-type and mutant paLDH were grown overnight in lysogeny medium with 100 μg/ml ampicillin at 37 °C and 200 rpm. Fifty milliliters of BL21 cell cultures were grown up to 0.6 $OD_{600\,nm}$ and induced with 0.8 mM IPTG (isopropyl β-D-1-thiogalactopyranoside) for 24 h, 20 °C, and 200 rpm to

express the enzymes. The induced cell cultures were harvested and lysed by BugBuster® (Merck Millipore, Billerica, USA), and subjected to Ni-NTA agarose column chromatography (Qiagen, Hilden, Germany) for enzyme purification. The enzyme purity was estimated by 12% SDS-PAGE and the concentration was measured by the Bradford assay [33].

Measuring Enzyme Activity

In vitro purified enzyme activity was assayed at 30 °C in 96-well plate with 50 mM sodium acetate buffer (pH 5.5); 0.2 mM NADH; 0.02~20 mM pyruvate, PPA, OB, or MOB as a substrate; and 0.1–2 μg of the purified enzyme. The oxidation rate of NADH was measured in triplicates by $UV_{340\ nm}$ absorbance with molar extinction coefficient of 6.22 mM^{-1} cm^{-1} (Molecular Devices, San Jose, USA). Specific activity was measured with 1.25 mM substrate. One unit of enzyme activity was defined as the amount of enzyme that oxidizes 1 μmol NADH per minute. Kinetic parameters were calculated by fitting the measured activity to Michaelis-Menten curves.

HPLC Analysis of Enzymatic Conversion of PPA into PLA

PPA was converted into PLA in vitro with the paLDH WT and mutants and analyzed by HPLC. A 3 ml reaction mixture consisted of 50 mM sodium acetate buffer (pH 6.5), 20 mM PPA, 1.5 mM NADH, and 18.6 nM of enzyme, and 30 mM sodium formate and 1 unit of formate dehydrogenase from *Candida boidinii* for in vitro cofactor regeneration of NADH. The mixture was sampled at 0, 0.5, 1, 2, 4, 8, and 12 h. The samples were then heat-inactivated at 99 °C, centrifuged for 5 min (13,000 rpm), and filtered by 0.2 μm Whatman PVDF filter (GE Healthcare, Pittsburgh, USA). YL9100 HPLC system (YL instruments, Anyang, Korea) installed with Aminex® HPX-87H Ion exclusion Column (300 mm × 7.8 mm) from Bio-Rad (Hercules, USA) and a UV detector at 210 nm was used to measure the conversion rate. Five millimolars of H_2SO_4 as a mobile phase at a flow rate of 0.6 ml min^{-1} was used, and the peaks for PPA and PLA were observed at 19.42 min and 41.28 min, respectively [10]. Chiralcel OJ-H column (250 mm × 0.46 mm, 5 μm) from Daicel (Tokyo, Japan) was used to distinguish the chiral D-PLA from L-PLA in the 12-h incubation sample [34]. The mobile phase consisted of hexane, 2-propanol and trifluoroacetic acid in 90:10:0.1 (*v*:*v*), and UV detection was at 261 nm. PPA was detected at 38 min, D-PLA at 29 min, and L-PLA at 34 min.

Result and Discussion

Homology Modeling and Rational Design of paLDH

The paLDH structure was homology modeled in silico from the crystal structure of *L. bulgaricus* D-LDH (PDB, 1j49) and validated by the Saves server, which includes Verify 3D, Errat, Prove, and Procheck modules (Supplementary Table S2). The model passed Verify 3D which determines the compatibility of an atomic model with its own amino acid sequence and comparing the results to good structures [35]. The overall model quality factor was 90% in Errat, which analyzes the statistics of non-bonded interactions between different atom types [36]. Prove calculating the volumes of atoms in macromolecules and *Z*-score deviation between the model, and highly resolved and refined PDB structures showed 3.7% buried

outlier protein atoms [37]. Procheck analyzed residue by residue and overall structure geometry with 99.7% of the residues in core or allowed regions in the Ramachandran plot, which is comparable to the 1.9% of the template [38]. Overall, the quality of the homology model was lower than that of the crystal structure of 1j49 but comparable with other homology models, and the few residues responsible were far from the active site that the model was eligible for docking simulation [27, 39].

The paLDH docked with pyruvate was used to predict residues for rational design of an enzyme with higher substrate specificity for PPA, OB, and MOB (Fig. 1). The carboxylic group of pyruvate is stabilized via hydrogen bonds with the main chain atoms of V77-G78 and the side chains of N76 and Y100. The 2-oxo group of pyruvate on the other hand faces R234 and H295 for stabilization and hydride transfer, respectively. The C_3 methyl group is in close proximity to F298 and Y51. This follows the reaction mechanism proposed by Razeto et al. [18]. A rational design strategy was coined as described in Table 1. N76, V77, and Y100 are changed into hydrophobic residues in varying size in order to examine the effect of bringing the substrate closer to the N76-G78 loop, which is expected to create more space for the substrate C_3 group, or exerting steric effect to push the substrate toward H295. F298 and Y51 are mutated into smaller hydrophobic residues to accommodate bulky hydrophobic functional group at C_3 of the substrate. R234 and H295 are excluded from the mutation candidate since they were reported to be crucial for catalytic mechanism [18, 40].

Screening of Mutants for Improved Activity on 2-Oxo Acids

The wild-type and rationally designed mutant paLDHs were screened for specific activity on pyruvate and other 2-oxo acids at 1.25 mM concentration (Fig. 2a). For pyruvate, the wild type showed the highest activity of 144.5 U mg^{-1}, while Y51L had the highest activity on PPA, OB, and MOB, each with 280, 32.1, and 14.0 U mg^{-1}, respectively. Y51I and Y51V also had higher specific activities than the wild type for PPA. F298I, V77A, and V77L mutants did not express in soluble form. N76A, N76V, N76L, V77I, and Y100F presented reduced activities than the wild type, and N76I, Y100L, Y100I, F298L, and F298V had negligible activities on all four substrates. Mutation of V77, although only its main chain atoms are used for hydrogen bond

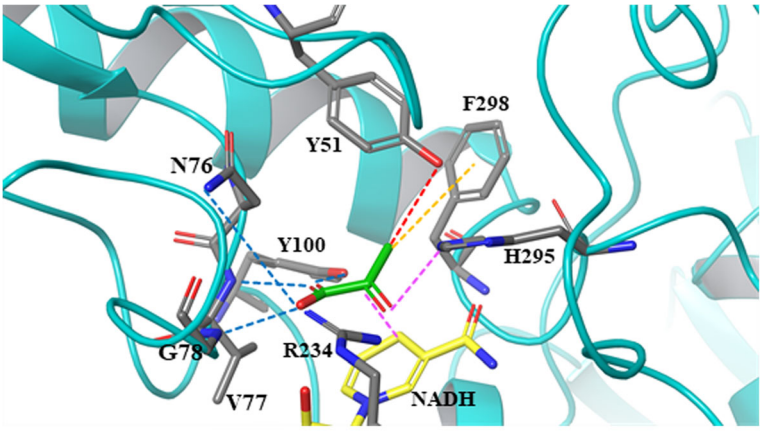

Fig. 1 The active site of paLDH docked with the substrate pyruvate (green), displaying the residues within 4 Å of the substrate as stick representation (gray). Blue dotted line, hydrogen bonds; orange dotted line, hydrophobic interaction; red dotted line, hydrophobic-hydrophilic contact; pink dotted line, hydride transfer distances

Table 1 Rational design strategy for paLDH

Residue	Substrate binding mode	Mutation strategy	Mutation
N76 V77 Y100	Form hydrogen bonds with the carboxylate group of 2-oxo acids via main chain (V77) and side chain (N76 and Y100)	Mutate selectively into hydrophobic residues to allow more space in the active site or sterically push the substrate toward the catalytic H295	N76A, N76V, N76L, N76I V77A, V77L, V77I Y100F, Y100L, Y100I
Y51 F298	Interact with the C_3 substituent functional group of 2-oxo acids	Mutate to smaller sized hydrophobic residues to accommodate large hydrophobic functional group at C_3	Y51L, Y51I, Y51V F298L, F298I , F298V
R234 H295	Involved directly in catalytic mechanism	Not selected as mutation target	Not applicable

formation to the substrate carboxylate group, had deleterious effect on the activity. N76 and Y100 mutations seem to have negative effects as the hydrogen bonds formed by their side chains are lost. F298 mutation into smaller hydrophobic residues was thought to reduce the steric hindrance on the C_3 group, but did not yield significant activity. Previous studies which mutated F298 also did not yield improvement in the activity for the four substrates [12, 21]. The result indicated Y51 is a key residue to increasing substrate specificity to 2-oxo acids, and further mutations of the residue into hydrophobic, hydrophilic, and aromatic residues were carried out (Fig. 2b). Y51F showed the highest specific activity for PPA, OB, and MOB among the Y51 mutants with 523, 51.1, and 41.5 U mg^{-1}, followed by Y51M and Y51L. Y51A and Y51S also show significant activities toward PPA but no other 2-oxo acids.

Kinetic Analysis of Improved Y51 Mutants

The wild type and Y51L, Y51M, Y51F, Y51A, and Y51S mutants of paLDH were analyzed for kinetic parameters (Table 2). The wild type had K_m of 2.6 mM for PPA, which was 6.5~16-fold higher than those of the Y51 mutants (0.16~0.40 mM), indicating significant improvement in substrate binding affinity via mutation. The k_{cat} values also increased from 41.3 s^{-1} of the wild type up to 462 s^{-1} for Y51M, and the k_{cat}/K_m was the highest with 2200 s^{-1} mM^{-1} for Y51L. This coincides with the previous works by Ishikura and Zheng which pointed the mutation of Y51 or equivalent residue into leucine presented the highest activity on PPA [11, 12]. Mutation into small hydrophobic alanine improved the K_m the most with 0.16 mM, but

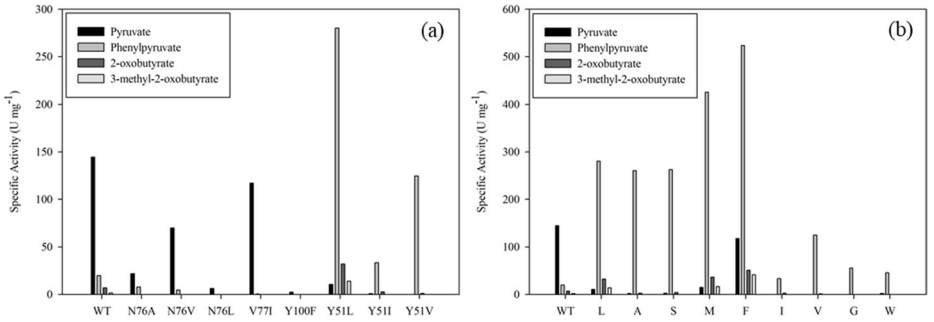

Fig. 2 The specific activities on pyruvate, PPA, OB, and MOB by (**a**) rationally designed paLDH mutants and (**b**) Y51 site-specific mutants

Table 2 Kinetic parameters of the wild-type and engineered paLDH

Substrate	Parameter	Wild type	Y51L	Y51M	Y51F	Y51A	Y51S
Phenyl pyruvate	K_m (mM)	2.6 ± 0.0	0.17 ± 0.01	0.22 ± 0.00	0.22 ± 0.07	0.16 ± 0.02	0.40 ± 0.11
	k_{cat} (s^{-1})	41.3 ± 1.3	376 ± 26	462 ± 4	391 ± 39	269 ± 14	239 ± 36
	k_{cat}/K_m (s^{-1} mM^{-1})	15.9 ± 0.5	2200 ± 20	2130 ± 20	1880 ± 90	1720 ± 90	612 ± 80
2-Oxo butyrate	K_m (mM)	11 ± 0	12 ± 2	7.5 ± 1.7	2.7 ± 0.3	N.D.	N.D.
	k_{cat} (s^{-1})	50.7 ± 0.4	199 ± 20	152 ± 10	99.4 ± 8.4	N.D.	N.D.
	k_{cat}/K_m (s^{-1} mM^{-1})	4.40 ± 0.10	16.8 ± 0.7	20.7 ± 3.4	37.2 ± 0.8	N.D.	N.D.
3-Methyl-2-oxo butyrate	K_m (mM)	38 ± 12	12 ± 0	8.6 ± 0.5	7.7 ± 0.0	N.D.	N.D.
	k_{cat} (s^{-1})	33.9 ± 8.8	90.2 ± 4.4	76.2 ± 0.2	179 ± 6	N.D.	N.D.
	k_{cat}/K_m (s^{-1} mM^{-1})	0.892 ± 0.063	7.41 ± 0.01	8.85 ± 0.51	23.2 ± 0.9	N.D.	N.D.

N.D. not determined as the specific activities were lower than that of the wild type

not the k_{cat}. Mutation into small hydrophilic serine improved the K_m than the wild type but not as much as hydrophobic amino acids, because PPA has hydrophobic group at C_3. In cases of OB and MOB which have smaller steric sizes than PPA, Y51F had the highest improvement in K_m (2.7 and 7.7 mM) and k_{cat}/K_m (37.2 and 23.2 s^{-1} mM^{-1}). Phenylalanine may best interact with the 2-carbon and 3-carbon moiety of OB and MOB, respectively, while allowing enough steric space, whereas alanine was better suited to the interaction with the phenyl ring of PPA in terms of K_m. Overall, the Y51L, Y51M, and Y51F mutants showed higher activities for PPA than wild-type D-LDHs from other species, and higher k_{cat} for OB and MOB although with larger K_m, making them eligible for efficient conversion at high substrate concentration [11, 23, 41].

Substrate Docking and Structural Studies on Y51 Mutants

In order to structurally account for the mutants with kinetic parameters higher than that of wild type, the substrates PPA (Fig. 3), OB (Fig. 4), and MOB (Fig. 5) were docked in silico and their Gibbs free energy of binding (ΔG_{bind}) and key distances (d_1, for hydride transfer between NADH and C_2; d_2, for hydride transfer between 2-oxo group and nitrogen of H295 side chain; d_3, between the closest heavy atoms of the substrate C_3 functional group and the residue 51 side chain) were analyzed (Table 3). ΔG_{bind} is correlated with the K_m and the d_1 and d_2 are related with the $k_{cat,}$ although the distances are not sole determinant and k_{cat} may be influenced by other factors such as dynamic motion of the enzyme or pKa values of H295 [40, 42]. The substrate configuration with productive binding modes, as proposed by crystal structure studies from *L. bulgaricus* D-LDH and *L. helveticus* D-LDH bound with substrate analogs, were selected among many substrate poses resulted from the docking [18].

For PPA, ΔG_{bind} of the wild type was − 4.85 kcal mol^{-1}, compared with more stable binding of Y51L, M, F, A, and S (− 5.57∼− 6.95 kcal mol^{-1}), which corresponds to the reduced K_m of the mutants. The d_1 and d_2 were similar in most of the variants, but the substrate binding orientation differs significantly. The mutants with higher k_{cat} tend to have shorter d_2 than those with lower k_{cat}. In the wild type, due to the steric hindrance and unfavorable hydrophilic-hydrophobic contact exerted by Y51 on the phenyl substituent of PPA, the whole PPA molecule is rotated by the axis of the C_1–C_2 bond (Fig. 3a). The hydrogen bonds provided by the N76 side chain amide group and the G78 main chain N to the substrate carboxylate are lost as a result. The Y51L and A maintained similar d_3 as in the wild type, and the less favorable hydrophilic-hydrophobic contact in the wild type was replaced by more favorable hydrophobic interaction (Fig. 3b, e). Y51F shows an aromatic T-shaped pi stacking between the two phenyl rings (Fig. 3d) [43]. Y51M had an increased d_3 value, as marked by slightly higher K_m (Fig. 3c). Hydrophilic serine at the position also brought an increase in K_m, although to a less degree than the wild type due to smaller steric size of serine than tyrosine (Fig. 3f). Hydrogen bonds between the carboxylate group and the N76-G78 loop were also maintained in Y51S.

ΔG_{bind} for OB correlates with the K_m, with the most stable binding by Y51F. For docking poses of OB, both oxygen atoms of the carboxylate group of the substrate are stabilized by V77 and G78 nitrogen in Y51F, whereas only single oxygen was stabilized in the wild type, Y51L and Y51M (Fig. 4). The d_2 were similar among all four variants, but the d_1 were shorter for Y51L, M, and F than the wild type in relation to their relatively higher k_{cat}. The d_3 are the same for the wild type and Y51F, but the phenylalanine contributes more than the tyrosine to the hydrophobic interaction. The d_3 for Y51L and Y51M with OB indicate they are farther

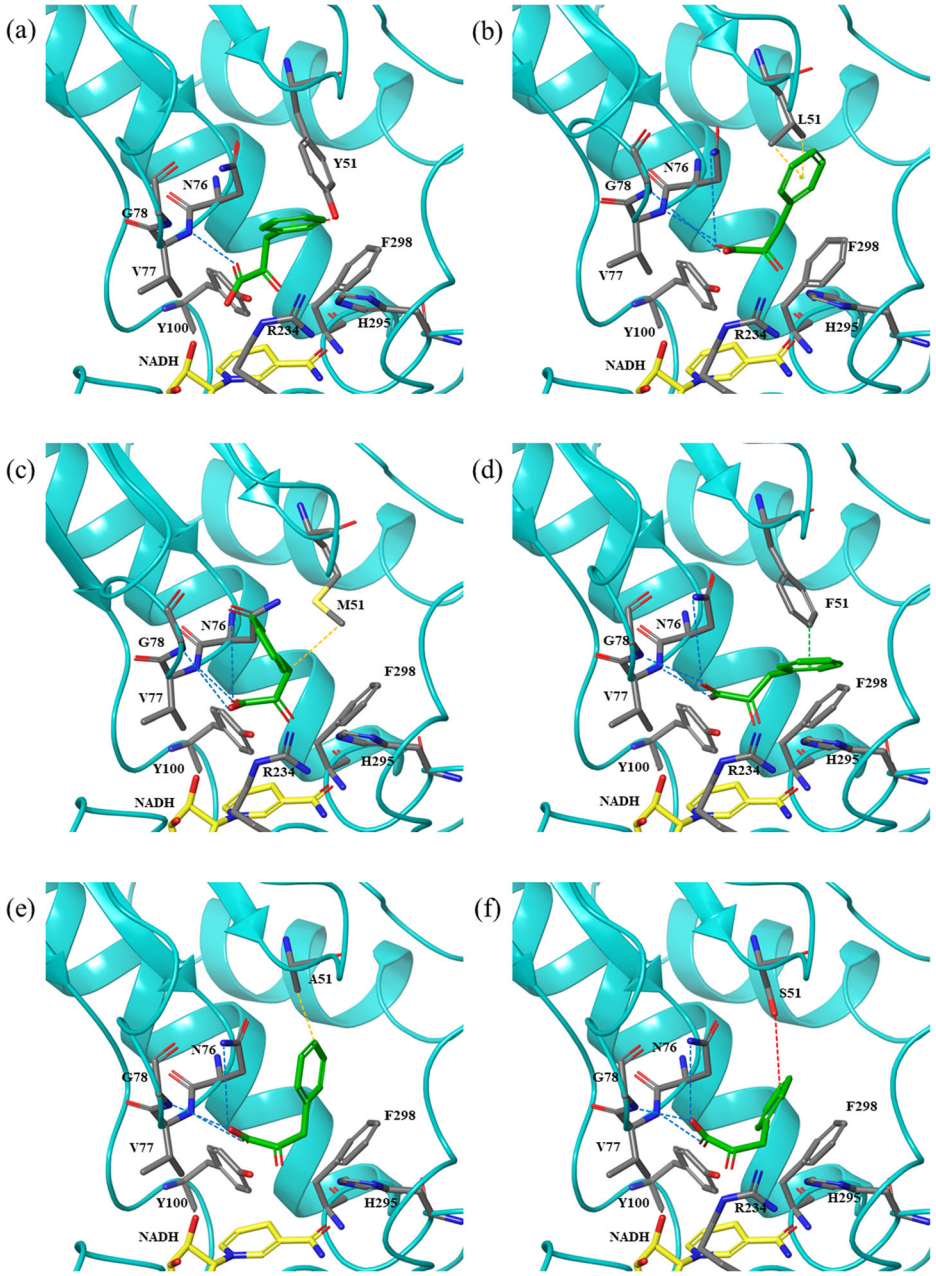

Fig. 3 The active site of the paLDH variants docked with the substrate PPA. The carbon atoms of NADH, substrates, and active site residues are colored in yellow, green, and gray, respectively. **a** Wild type. **b** Y51L. **c** Y51M. **d** Y51F. **e** Y51A. **f** Y51S. Blue dotted line, hydrogen bonds; orange dotted line, hydrophobic interaction; red dotted line, hydrophobic-hydrophilic contact; green dotted line, pi-pi stacking

away from the substrate's C_3 substituent, and the contribution on the hydrophobic interaction is less than that of Y51F.

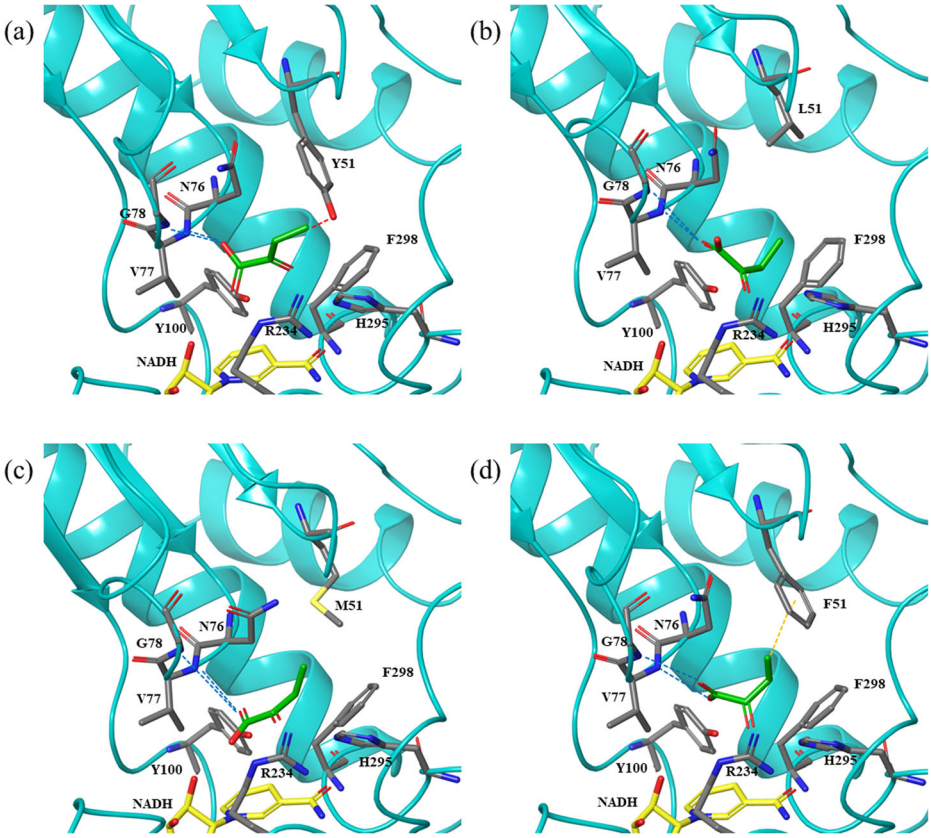

Fig. 4 The active site of the paLDH variants docked with OB. The carbon atoms of NADH, substrates, and active site residues are colored in yellow, green, and gray, respectively. **a** Wild type. **b** Y51L. **c** Y51M. **d** Y51F. Blue dotted line, hydrogen bonds; orange dotted line, hydrophobic interaction; red dotted line, hydrophobic-hydrophilic contact

The ΔG_{bind} for MOB also follows the K_m value, and the Y51F has the lowest ΔG_{bind} and K_m. The d_2 were similar among all the variants while d_1 decreased for the mutants as well as increased k_{cat}. The d_3 also indicate that given a similar distance, the hydrophobic Y51L and Y51M interact more favorably than the hydrophilic Y51 of the wild type, and Y51F with its hydrophobicity and proximity to MOB's C_3 substituent can contribute the most favorable to the interaction (Fig. 5). Overall, it was important to place hydrophobic residues in close distance to the hydrophobic C_3 substituent of the substrate to optimize the interaction and therefore increasing the activity. Overall, while the d_2 seem to be relatively invariable among the mutants and substrates, d_1 and d_3 were related to the increased catalytic efficiencies, indicating the importance of the type and the distance of the interaction the residue 51 side chain provides.

HPLC Analysis of Enzymatic Conversion of PPA into PLA

Since PPA has a practical significance in the industrial application, in vitro enzymatic conversion of PPA into PLA was investigated. The paLDH mutants with a high catalytic

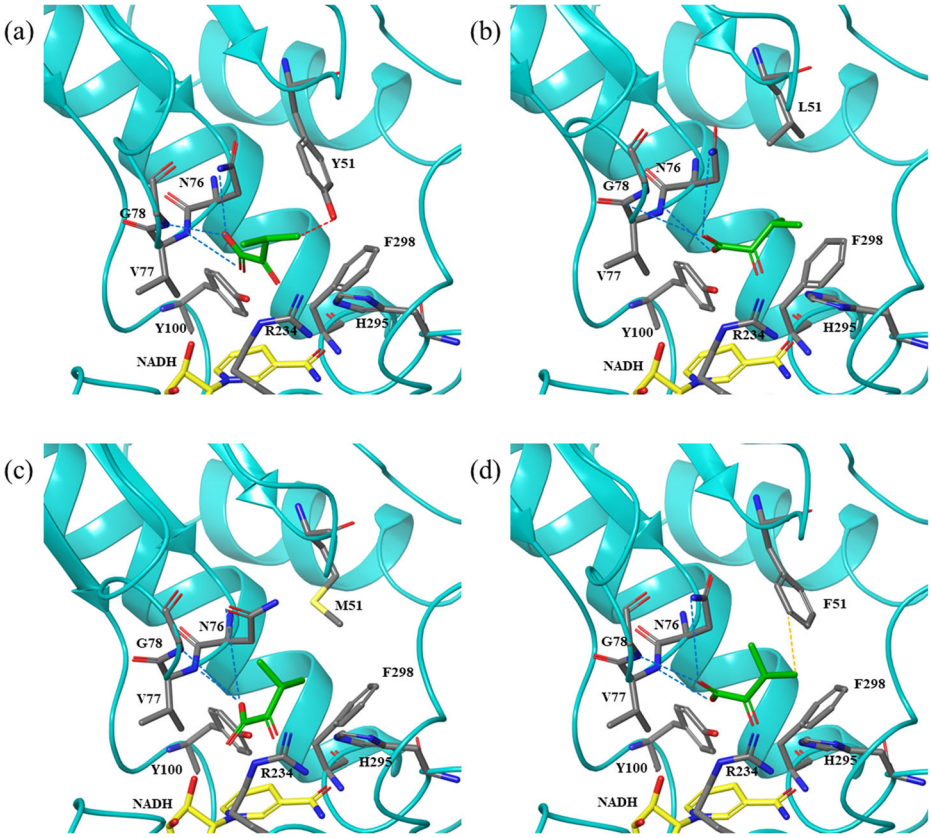

Fig. 5 The active site of the paLDH variants docked with MOB. The carbon atoms of NADH, substrates, and active site residues are colored in yellow, green, and gray, respectively. **a** Wild type. **b** Y51L. **c** Y51M. **d** Y51F. Blue dotted line, hydrogen bonds; orange dotted line, hydrophobic interaction; red dotted line, hydrophobic-hydrophilic contact

Table 3 Docking parameters for PPA, OB, or MOB as a substrate in paLDH variants

Substrate	paLDH	ΔG_{bind} (kcal mol^{-1})	d_1 (Å)	d_2 (Å)	d_3 (Å)
PPA	WT	−4.85	4.5	2.9	4.0
	Y51L	−6.72	4.8	2.7	3.8
	Y51M	−6.22	4.9	2.6	5.6
	Y51F	−6.95	4.5	2.7	3.9
	Y51A	−6.46	4.2	3.0	4.3
	Y51S	−5.57	4.3	3.7	3.5
OB	WT	−4.79	5.0	2.8	3.8
	Y51L	−4.40	4.2	2.9	5.6
	Y51M	−5.77	4.2	2.9	4.7
	Y51F	−6.13	4.4	2.8	3.8
MOB	WT	−4.85	5.1	2.8	4.7
	Y51L	−5.68	5.0	2.7	4.4
	Y51M	−5.78	4.4	2.9	4.6
	Y51F	−6.12	4.6	2.8	3.5

ΔG_{bind}, binding free energy between substrate and the enzyme; d_1, the distance between the NADH and the substrate C_2; d_2, the distance between the H295 side chain N atom and the substrate 2-oxo group; d_3, the distance between closest heavy atoms of the side chain of the residue 51 and the substrate C_3 substituent group

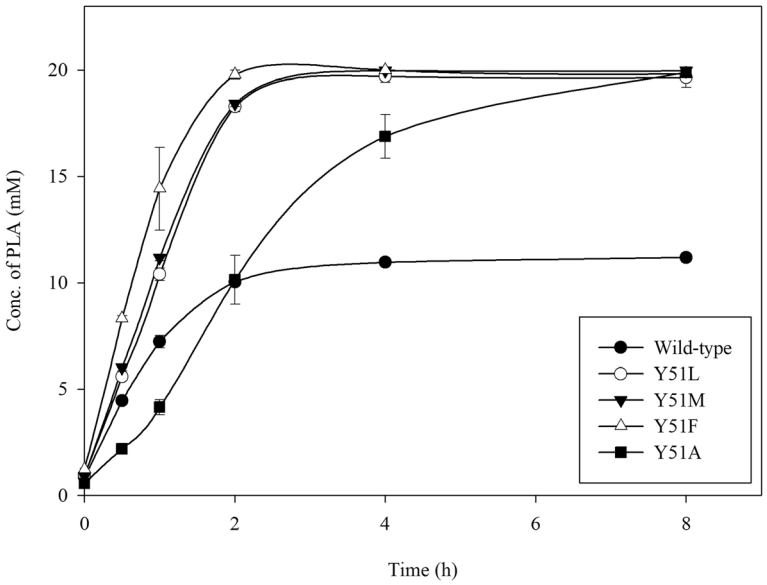

Fig. 6 In vitro enzymatic conversion of PPA into PLA by paLDH variants

efficiency, namely Y51L, M, F, and A, revealed the highest productivity was found with the Y51F, closely followed by Y51M and L (Fig. 6). All mutants reached over 98% conversion within the time window of 8 h, but the wild type with a maximum of 56% conversion. Y51F reached 98% conversion within 2 h, for a productivity of 1.61 g^{-1} L^{-1} h^{-1}. The kinetic parameters indicated Y51L or Y51M as the most promising mutant, but the Y51F is better-suited for the conversion at high concentrations of PPA, because Y51L has an activity decrease over 0.3 mM and Y51M over 0.6 mM of the substrate concentration (Supplementary Fig. S2). Chiral HPLC detected only a peak at 29 min but not at 34 min for the mutants, indicating over 99% of the product is enantiomerically pure D-form (Supplementary Fig. S3). The wild type and Y51A showed peaks at 38 min, which correspond to the unreacted PPA.

Conclusion

Engineering the D-LDH from *P. acidilactici* for substrate specificity and higher activity on PPA, OB, and MOB via rational design and site-directed mutagenesis successfully yielded several Y51 mutants. The Y51F mutant had the highest activity on OB and MOB, and the highest conversion on PPA. Y51L and Y51M, although with high catalytic efficiencies on PPA, exhibited decreasing activities at higher substrate concentrations that led to limitations in in vitro bioconversion of PPA. The structural study can provide an effective engineering strategy to catalyze 2-oxo acids with varying sizes of C_3 substituents.

Funding Information This research was supported by the Technology Development Program to Solve Climate Changes of the National Research Foundation (NRF) funded by the Ministry of Science and ICT (Grant Number, 2017M1A2A2087630).

Compliance with Ethical Standards

Conflict of Interest The authors declare that they have no conflicts of interest.

Research Involving Human Participants and/or Animals This article does not contain any studies with human participants performed by any of the authors.

References

1. Taguchi, H., & Ohta, T. (1991). D-lactate dehydrogenase is a member of the D-isomer-specific 2-hydroxyacid dehydrogenase family. Cloning, sequencing, and expression in Escherichia coli of the D-lactate dehydrogenase gene of Lactobacillus plantarum. *The Journal of Biological Chemistry, 266*(19), 12588–12594.
2. Kutzenko, A. S., Lamzin, V. S., & Popov, V. O. (1998). Conserved supersecondary structural motif in NAD-dependent dehydrogenases. *FEBS Letters, 423*(1), 105–109.
3. Södergård, A., & Stolt, M. (2002). Properties of lactic acid based polymers and their correlation with composition. *Progress in Polymer Science, 27*(6), 1123–1163.
4. Tsuji, H., & Okumura, A. (2010). *Polymer Journal, 43*, 317.
5. Cheong, S., Clomburg, J. M., & Gonzalez, R. (2018). A synthetic pathway for the production of 2-hydroxyisovaleric acid in Escherichia coli. *Journal of Industrial Microbiology & Biotechnology, 45*(7), 579–588.
6. Fujita, T., Nguyen, H. D., Ito, T., Zhou, S., Osada, L., Tateyama, S., Kaneko, T., & Takaya, N. (2013). Microbial monomers custom-synthesized to build true bio-derived aromatic polymers. *Applied Microbiology and Biotechnology, 97*(20), 8887–8894.
7. Lavermicocca, P., Valerio, F., & Visconti, A. (2003). Antifungal activity of phenyllactic acid against molds isolated from bakery products. *Applied and Environmental Microbiology, 69*(1), 634–640.
8. Chaudhari, S. S., & Gokhale, D. V. (2016). *Journal of Bacteriology & Mycology, 2*, 121–125.
9. Tokuda, C., Ishikura, Y., Shigematsu, M., Mutoh, H., Tsuzuki, S., Nakahira, Y., Tamura, Y., Shinoda, T., Arai, K., Takahashi, O., & Taguchi, H. (2003). Conversion of Lactobacillus pentosus D-lactate dehydrogenase to a D-hydroxyisocaproate dehydrogenase through a single amino acid replacement. *Journal of Bacteriology, 185*(16), 5023–5026.
10. Zhu, Y., Hu, F., Wang, L., & Qi, B. (2015). Enhancement of phenyllactic acid biosynthesis by recognition site replacement of D-lactate dehydrogenase from Lactobacillus pentosus. *Biotechnology Letters, 37*(6), 1233–1241.
11. Ishikura, Y., Tsuzuki, S., Takahashi, O., Tokuda, C., Nakanishi, R., Shinoda, T., & Taguchi, H. (2005). Recognition site for the side chain of 2-ketoacid substrate in D-lactate dehydrogenase. *Journal of Biochemistry, 138*(6), 741–749.
12. Zheng, Z., Sheng, B., Gao, C., Zhang, H., Qin, T., Ma, C., & Xu, P. (2013). Highly stereoselective biosynthesis of (R)-α-hydroxy carboxylic acids through rationally re-designed mutation of d-lactate dehydrogenase. *Scientific Reports, 3*(1), 3401.
13. Mu, W., Yu, S., Jiang, B., & Li, X. (2012). Characterization of d-lactate dehydrogenase from Pediococcus acidilactici that converts phenylpyruvic acid into phenyllactic acid. *Biotechnology Letters, 34*(5), 907–911.
14. Yu, S., Jiang, H., Jiang, B., & Mu, W. (2012). Characterization of D-lactate dehydrogenase producing D-3-phenyllactic acid from Pediococcus pentosaceus. *Bioscience Biotechnology and Biochemistry, 76*(4), 853–855.
15. Steiner, K., & Schwab, H. (2012). Recent advances in rational approaches for enzyme engineering. *Computational and Structural Biotechnology Journal, 2*(3), e201209010.
16. Yeon, Y. J., Park, H. Y., & Yoo, Y. J. (2015). Engineering substrate specificity of succinic semialdehyde reductase (AKR7A5) for efficient conversion of levulinic acid to 4-hydroxyvaleric acid. *Journal of Biotechnology, 210*, 38–43.
17. Yeon, Y. J., Park, H. Y., & Yoo, Y. J. (2013). Enzymatic reduction of levulinic acid by engineering the substrate specificity of 3-hydroxybutyrate dehydrogenase. *Bioresource Technology, 134*, 377–380.
18. Razeto, A., Kochhar, S., Hottinger, H., Dauter, M., Wilson, K. S., & Lamzin, V. S. (2002). Domain closure, substrate specificity and catalysis of d-lactate dehydrogenase from Lactobacillus bulgaricus. *Journal of Molecular Biology, 318*(1), 109–119.
19. Antonyuk, S. V., Strange, R. W., Ellis, M. J., Bessho, Y., Kuramitsu, S., Inoue, Y., Yokoyama, S., & Hasnain, S. S. (2009). Structure of D-lactate dehydrogenase from Aquifex aeolicus complexed with NAD+ and lactic acid (or pyruvate). *Acta Crystallographica. Section F, Structural Biology and Crystallization Communications, 65*(12), 1209–1213.
20. Hammes-Schiffer, S. (2002). Comparison of hydride, hydrogen atom, and proton-coupled electron transfer reactions. *ChemPhysChem., 3*(1), 33–42.

21. Wang, M., Zhu, L., Xu, X., Wang, L., Yin, R., & Yu, B. (2016). Efficient production of enantiomerically pure d-phenyllactate from phenylpyruvate by structure-guided design of an engineered d-lactate dehydrogenase. *Applied Microbiology and Biotechnology, 100*(17), 7471–7478.
22. Dengler, U., Niefind, K., Kiess, M., & Schomburg, D. (1997). Crystal structure of a ternary complex of d -2-hydroxyisocaproate dehydrogenase from Lactobacillus casei , NAD + and 2-oxoisocaproate at 1.9 Å resolution 1 1Edited by R. Huber. *Journal of Molecular Biology, 267*(3), 640–660.
23. Lee, H. S., Park, J., Yoo, Y. J., & Yeon, Y. J. (2019). A novel d-2-hydroxy acid dehydrogenase with high substrate preference for phenylpyruvate originating from lactic acid bacteria: structural analysis on the substrate specificity. *Enzyme and Microbial Technology, 125*, 37–44.
24. Altschul, S. F., Madden, T. L., Schaffer, A. A., Zhang, J., Zhang, Z., Miller, W., & Lipman, D. J. (1997). Gapped BLAST and PSI-BLAST: a new generation of protein database search programs. *Nucleic Acids Research, 25*(17), 3389–3402.
25. Prime. (2018). *Schrödinger Release 2018-4, Schrödinger*. New York, NY: LLC.
26. Lovell, S. C., Davis, I. W., Arendall, W. B., 3rd, De Bakker, P. I., Word, J. M., Prisant, M. G., Richardson, J. S., & Richardson, D. C. (2003). Structure validation by Cα geometry: ϕ, ψ and Cβ deviation. *Proteins., 50*(3), 437–450.
27. Pramanik, K., Ghosh, P. K., Ray, S., Sarkar, A., Mitra, S., & Maiti, T. K. (2017). An in silico structural, functional and phylogenetic analysis with three dimensional protein modeling of alkaline phosphatase enzyme of Pseudomonas aeruginosa. *Journal, Genetic Engineering & Biotechnology, 15*(2), 527–537.
28. LigPrep. (2018). *Schrödinger Release 2018–4, Schrödinger*. New York, NY: LLC.
29. Friesner, R. A., Banks, J. L., Murphy, R. B., Halgren, T. A., Klicic, J. J., Mainz, D. T., Repasky, M. P., Knoll, E. H., Shelley, M., Perry, J. K., Shaw, D. E., Francis, P., & Shenkin, P. S. (2004). Glide: a new approach for rapid, accurate docking and scoring. 1. Method and assessment of docking accuracy. *Journal of Medicinal Chemistry, 47*(7), 1739–1749.
30. Halgren, T. A., Murphy, R. B., Friesner, R. A., Beard, H. S., Frye, L. L., Pollard, W. T., & Banks, J. L. (2004). Glide: a new approach for rapid, accurate docking and scoring. 2. Enrichment factors in database screening. *Journal of Medicinal Chemistry, 47*(7), 1750–1759.
31. Glide. (2018). *Schrödinger Release 2018-4*. New York, NY: Schrödinger.
32. Zheng, L., Baumann, U., & Reymond, J. L. (2004). An efficient one-step site-directed and site-saturation mutagenesis protocol. *Nucleic Acids Research, 32*(14), e115.
33. Bradford, M. M. (1976). A rapid and sensitive method for the quantitation of microgram quantities of protein utilizing the principle of protein-dye binding. *Analytical Biochemistry, 72*(1-2), 248–254.
34. Tekewe, A., Singh, S., Singh, M., Mohan, U., & Banerjee, U. C. (2008). Development and validation of HPLC method for the resolution of drug intermediates: dl-3-Phenyllactic acid, dl-O-acetyl-3-phenyllactic acid and (±)-mexiletine acetamide enantiomers. *Talanta., 75*(1), 239–245.
35. Luthy, R., Bowie, J. U., & Eisenberg, D. (1992). Assessment of protein models with three-dimensional profiles. *Nat., 356*(6364), 83–85.
36. Colovos, C., & Yeates, T. O. (1993). Verification of protein structures: patterns of nonbonded atomic interactions. *Protein Science, 2*(9), 1511–1519.
37. Pontius, J., Richelle, J., & Wodak, S. J. (1996). Deviations from standard atomic volumes as a quality measure for protein crystal structures. *Journal of Molecular Biology, 264*(1), 121–136.
38. Laskowski, R. A., Rullmannn, J. A., Macarthur, M. W., Kaptein, R., & Thornton, J. M. (1996). AQUA and PROCHECK-NMR: programs for checking the quality of protein structures solved by NMR. *Journal of Biomolecular NMR, 8*(4), 477–486.
39. Kumar, A., Kumar, S., Kumar, A., Sharma, N., Sharma, M., Pal Singh, K., & Rathore, M. (2017). *Proc Natl Acad Sci, India, Sect B Biol Sci, 88*, 1539–1548.
40. Taguchi, H., Ohta, T., & Matsuzawa, H. (1997). Involvement of Glu-264 and Arg-235 in the essential interaction between the catalytic imidazole and substrate for the D-lactate dehydrogenase catalysis. *Journal of Biochemistry, 122*(4), 802–809.
41. Furukawa, N., Miyanaga, A., Togawa, M., Nakajima, M., & Taguchi, H. (2014). Diverse allosteric and catalytic functions of tetrameric d-lactate dehydrogenases from three Gram-negative bacteria. *AMB Express, 4*(1), 76.

42. Zhadin, N., Gulotta, M., & Callender, R. (2008). Probing the role of dynamics in hydride transfer catalyzed by lactate dehydrogenase. *Biophysical Journal, 95*(4), 1974–1984.
43. Sinnokrot, M. O., Valeev, E. F., & Sherrill, C. D. (2002). Estimates of the ab initio limit for π–π interactions: the benzene dimer. *Journal of the American Chemical Society, 124*(36), 10887–10893.

Affiliations

Hoe-Suk Lee[1] · Jisu Park[2] · Young Je Yoo[1,3] · Young Joo Yeon[2]

Hoe-Suk Lee
hsl0828@snu.ac.kr

Jisu Park
jspark@gwnu.ac.kr

[1] Program of Bioengineering, Seoul National University, 1 Gwanak-ro, Gwanak-gu, Seoul 08826, Republic of Korea

[2] Department of Biochemical Engineering, Gangneung-Wonju National University, 7, Jukheon-gil, Gangneung-si, Gangwon-do 25457, Republic of Korea

[3] School of Chemical and Biological Engineering, Seoul National University, 1 Gwanak-ro, Gwanak-gu, Seoul 08826, Republic of Korea